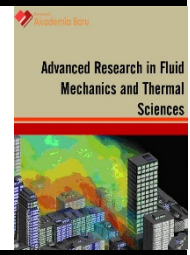




Journal of Advanced Research in Fluid Mechanics and Thermal Sciences

Journal homepage: www.akademiabaru.com/arfmmts.html
ISSN: 2289-7879



Open
Access

Validation of a benchmark methanol flame using OpenFOAM

Mohd Fairus Mohd Yasin^{1,*}, Stewar Cant², Mohammad Arqam¹

¹ Fakulti Kejuruteraan Mekanikal, Univeristi Teknologi Malaysia, 81310 UTM Skudai, Johor, Malaysia

² Department of Engineering, University of Cambridge, Trumpington St, Cambridge CB2 1PZ, United Kingdom

ARTICLE INFO

Article history:

Received 16 October 2016

Received in revised form 25 November 2016

Accepted 30 November 2016

Available online 8 December 2016

ABSTRACT

The spray combustion simulation includes the modelling of many physical processes that interact with each other such as droplet breakup, evaporation, mixing, and reaction which pose a challenge to the modelling effort. The present study evaluates the accuracy of an unsteady spray combustion solver based on a benchmark methanol spray combustion database. Extensive validation has been done to evaluate the accuracy of the models and improvements to the state-of-the-art of spray combustion model are proposed. A monocomponent fuel, methanol is chosen due to its well established physical and chemical properties. A comprehensive boundary condition for spray is modelled in OpenFOAM to capture the size and velocity of different droplet groups in the radial direction near the burner. A qualitative validation of the global spray-combustion characteristics along with a quantitative validation of the gas phase velocity and droplet size show a good agreement between the simulation and the experiment. The overpredicted inter-phase momentum transfer is observed in the velocity prediction of the gas phase and further supported by the overprediction of the droplet drag. The modified RNG $k - \epsilon$ model shows an enhanced capability in predicting the gas velocity profile in the near-field.

Keywords:

Methanol, Modelling, CFD, Validation,
Spray, Flame

Copyright © 2016 PENERBIT AKADEMIA BARU - All rights reserved

1. Introduction

Improving the accuracy of CFD requires model development and validation based on the identified weaknesses in the model. Though many simplified cases such as the single droplet breakup and evaporation have been studied experimentally and numerically, the same phenomena in sprays need to be addressed. The validation of spray combustion characteristics with a complex swirling flow is at the current limits of CFD which requires among others, the refinement in the spray boundary condition, and the turbulence modelling. Validation of the predicted spray characteristics based on the phase doppler anemometry measurement has to be done using a Lagrangian post-processor. Due to the complex interaction between different spray-combustion models, the validation of simplified cases such as the non-evaporating spray and the monocomponent fuel spray are needed to achieve an overall improvement in the reacting spray simulation [1].

* Corresponding author.

E-mail address: mohdfairus@mail.fkm.utm.my (Mohd Fairus Mohd Yasin)

Three different approaches of modelling turbulent flow are the Direct Numerical Simulation (DNS), the Large Eddy Simulation (LES), and the Reynolds Averaged Navier Stokes (RANS). Due to a prohibitively large computational cost of DNS to resolve all time and length scales in a flow, the LES and RANS become more practical. Several studies have model reacting sprays using LES [2], which offers useful insights about the unsteady phenomena such as ignition, blow-off, and combustion instability. RANS which solves the mean velocity field and model the turbulent fluctuation has been the most widely used for design purposes. Since the present study focuses on steady combustion processes that requires the implementation of the advanced spray models (breakup and evaporation models), the RANS approach is chosen. In the present study, a variant of the RANS method called Unsteady Reynolds Averaged Navier Stokes (URANS) [3, 4] which solve the Reynolds averaged equations in three dimensions with time dependence is chosen.

The validation of spray combustion simulations has been limited due to the complex interplay between different physical processes and the scarcity of reliable data. Most of the validation studies of unsteady spray combustion simulations have been limited to the macro characteristics such as the spray penetration, spray shape, flame shape, and global droplet size [5, 6]. A satisfactory validation of the micro characteristics such as local droplet size, droplet flux, and velocity profiles which is more practically done using a steady spray configuration has been reported in spray of a single component fuel (methanol) [7, 8]. A previous study has validated the spray-combustion characteristic of a biodiesel spray in a lab-scale burner using the real properties of biodiesel and discrete multicomponent model for droplets evaporation [17]. Another study employs the same validation case using FLUENT® to study the atomisation and the combustion model [9].

In the present study, the spray combustion characteristics of a monocomponent fuel will be simulated based on detailed boundary conditions using empirical data. A special care is taken in the specification of spray boundary condition to ensure the statistical accuracy of droplet size and velocity in the experiment is reproduced. The predictions of the local gas phase velocity and the spray characteristics will be carefully compared with the experimental data to investigate the accuracy of spray and turbulence models.

2. Experimental and numerical conditions

A confined swirl-stabilised burner with an injector nozzle and swirler exit near the bottom is used in the experiment as shown in Figs. (a) and (b)[7]. The exhaust outlet is at the side which is near top of the burner.

A swirling air flow is produced through a 12 vane swirl cascade and liquid methanol is injected through a pressure swirl atomiser. The injector is located at the center of the swirler outlet (annulus) near which the flame is stabilised. Table 1 provides the experimental conditions at atmospheric pressure. The radial profiles of droplet size, velocity, droplet density, and volume flux are measured using phase Doppler interferometry at 10 mm intervals from the axial location $z = 5$ mm to $z = 65$ mm from the injector nozzle.

The present study begins with a standard URANS spray combustion solver implemented within the OpenFOAM-1.6 library. The standard solver includes an Eulerian-Lagrangian two phase formulation in which the continuous phase is treated using the mesh-based Eulerian method while the dispersed phase is tracked over time using the Lagrangian method. An Euler implicit time integration method is employed together with the Pressure Implicit Split Operator (PISO) velocity-pressure coupling procedure [10].

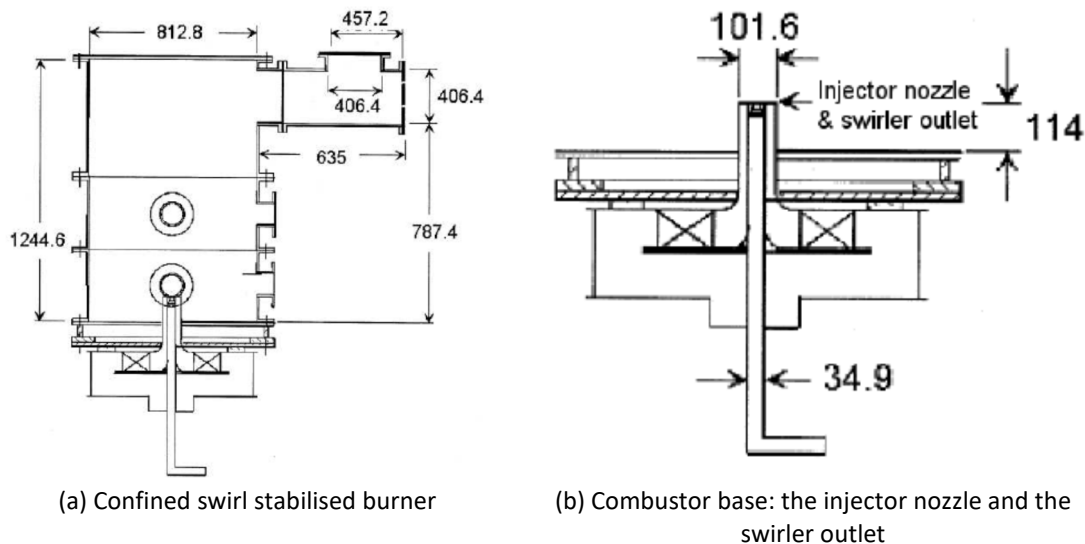


Fig. 1. Schematic diagrams of the confined swirl stabilised burner. All dimensions are in mm. Adapted from [7].

In the present simulation, 100000 structured hexahedral cells are clustered near the injector where the swirler is treated as the inlet in the simulation. A cell size of 2.5 mm is deemed adequate based on a separate mesh independence study. A cylindrical geometry with 300 mm length and 180 mm diameter is considered suitable to capture the 300 mm height and 50 mm radial width of the experimental flame [80]. The truncated geometry provides an affordable computation time for the present simulation of a reacting flow. The pressure at the outlet of the computational domain is assumed to be atmospheric. The boundary conditions of the gas phase inlet in the non-reacting and reacting cases are taken from two measurement sets of the three component velocities at $z = 1.4$ mm in the respective cases. The turbulence length scale is assumed to be 10% of the vane height. The turbulence intensity profiles are observed to have high gradient near the wall due to the velocity fluctuation induced by the wall.

The spray boundary condition is set at $z = 5$ mm which is the most upstream location of the droplet size measurement. At the location of the spray boundary condition, 10 initial spray distributions corresponding to the 10 radial locations of the PDI measurement are implemented. Based on two PDI point measurements, the characteristic diameter δ and spread parameter n of the droplet size pdf are calculated. A profile of mean injection velocity is implemented based on 10 measured mean axial and radial velocities of the droplets at respective locations of the initial spray. The cone angle of each injector is determined based on the assumption that the droplets follow straight line trajectories from the injector nozzle location at $z = 0$ mm to the spray boundary condition. The measured volume flux profile is then used to determine the number of injected computational parcels per time step and the mass flow rates of each initial spray distribution. The integral mass flow rate of all initial spray distributions is fixed to conserve the fuel mass flow rate of the experiment. The spray is represented by 70000 computational parcels at steady state and requires 36 hours average CPU time with 8 processors on an Intel Xeon® E5620 (2.4GHz processor).

A 2-step reaction mechanism of methanol that includes CO species [10] with respective Arrhenius reaction rate parameters as shown in Table 2. The baseline case implements the renormalisation group method (RNG) model for the turbulent flow and the Partially Stirred Reactor Model (PaSR) model for turbulence-chemistry interaction [11]. A standard d^2 model and a rigid sphere drag model [12] are implemented to simulate droplet evaporation and drag respectively.

Table 1

The experimental conditions of the methanol spray flame [7] where v_{air} the volume flow rate of air is

m_{fuel} (kg/hr)	3
v_{air} (m ³ /hr)	56.7
fuel temperature (K)	293
air temperature (K)	293
equivalence ratio	0.3
vane angle	50°
swirl number	0.58

Table 2

CH₃OH Rate constants as implemented in the present simulation where $k = AT^n \exp(-E/RT)$ where A, n, E, R and T are pre-exponential factor, temperature exponent, activation energy, universal gas constant, and temperature respectively. Units are in cm, mole, and sec [11].

Reaction	A	n	E (kcal/mole)
$CH_3OH + O_2 \rightarrow CO + 2H_2O$	3.70×10^{12}	0.0	30000.0
$CO + 0.5O_2 + H_2O \leftrightarrow CO_2 + H_2O$	3.98×10^{14}	0.0	40000.0

3. Results and analysis

Fig. 1(a) and (b) show the experimental flame image and the predicted temperature field respectively with the swirler outlet annulus included in each figure. The experimental flame image visualises the line of sight flame image and a cross section visualisation of the spray that is made visible through a laser sheet illumination [7].

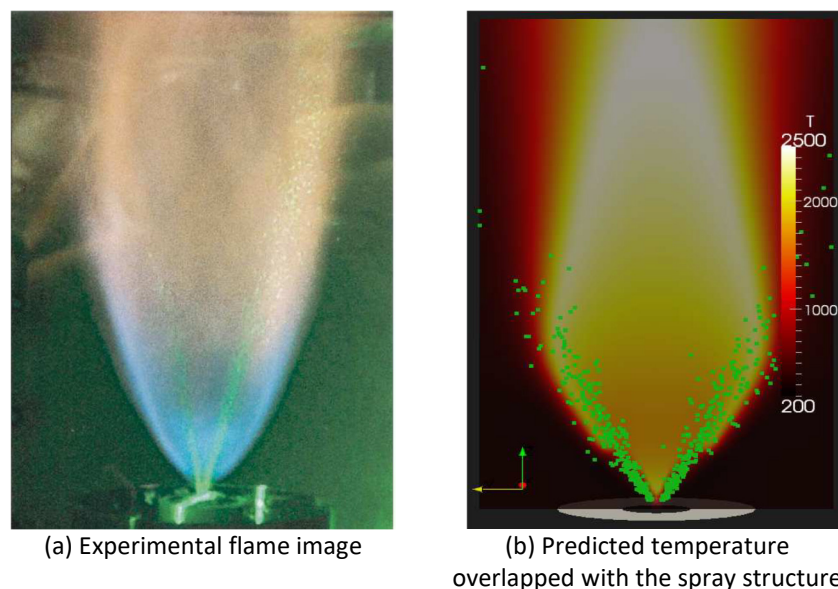


Fig. 1. Comparison between the simulated methanol spray flame (baseline) and that of the experiment

The height of experimental flame is not specifically mentioned in the respective literature though a 300 mm flame height is reported elsewhere [8] through a visual observation in the experiment. Referring to Fig. 1(b) both the predicted temperature field and spray structure lie on a cross section plane which is parallel to the direction of the flow with a height of 300 mm.

The weak swirling air from the annulus at the bottom promotes the mixing between the fuel and oxidiser and stabilises the candle-like flame near the injector nozzle. The expansion of the flame brush to about the size of the swirler outlet in the experiment is reproduced in the simulation with the spray cone angle located within the high temperature region. Due to a rapid evaporation within the spray core, a low temperature fuel-rich region is produced in the lower part of the predicted temperature field and the flame front is stabilised within the shear layer of the spray a few millimeters downstream of the nozzle. The visual observation in the experiment indicates a flame lift between 5 mm to 10 mm [7]. A high temperature region is predicted towards the top of the flame brush where the evaporation of fuel droplets is already completed.

The modelling of swirl flow is affected by the implementation of different turbulence models. Three turbulence models are investigated: the modified RNG (baseline), the standard RNG, and the standard $k - \varepsilon$ models. The C_2 constant that occurs in the transport equation of dissipation rate is one of the empirically derived constants in the standard $k - \varepsilon$ model [13]. In the standard RNG model, the same constant is analytically derived based on the RNG theory [14]. In the modified RNG model, the value of C_2 is chosen based on the validation of the velocity profiles in the non-reacting flow as will be discussed in subsequent paragraphs. For both RNG models, the turbulent Prandtl number for the thermal diffusivity calculation is assumed to be 0.6 while the standard $k - \varepsilon$ model maintains the original value of 1.0. Other constants of the RNG and $k - \varepsilon$ models follow the standard form stated in the original references [13,14]. A comparison of the turbulence model C_2 constant is included in Table 3.

Table 3
Comparison of the C_2 constants of different turbulence model

	modified RNG	standard RNG	standard $k-\varepsilon$
C_2	3.5	1.68	1.92

Figure 3(a) to (f) shows the validation against the experimental data for the three-component velocity profile in the radial direction where the radial location \hat{r}_{ch} is normalised with respect to the maximum radial location where the droplet is detected in the experiment. Fig. 3(a) and (b) show that a uniform profile of the far field ($\hat{r}_{ch} > 0.4$) axial velocity due to the thermal expansion is reproduced quite well in the baseline case using the modified RNG $k - \varepsilon$ model. The shift in the maximum tangential velocity locations of the reacting case (Fig. 3 (c) and (d)) towards the near field ($\hat{r}_{ch} < 0.4$) region due to the change in the far field axial velocity region of the two cases is predicted. Based on the measured velocity profiles, the spray dynamics show visible effects on the gas velocity components. However, the same effect is over predicted as can be seen in all the three component velocities in the near field region. Large discrepancies between the predicted and measured velocity in that region can be seen in the axial and radial velocity profiles. In contrast, the trend of the tangential velocity prediction in the near field region agrees quite well with that of the experiment. This is partly because the velocity vectors of the injected droplet at the spray boundary condition do not include the tangential components. After the injection, droplets are influenced by the tangential velocity of the swirling air due to the inter-phase momentum coupling. The over predicted effect of the spray dynamics on the gas velocity is due to the over predicted inter-phase momentum transfer which is coupled to the momentum transport equation of the gas phase through the respective source term. The issue of the mesh dependence of the inter-phase point source term that is highlighted elsewhere [15] may not cause the over predicted spray dynamics effect on the gas phase because the issue is only observed in the momentum transport equation with no similar observation in the mass and energy transport equations.

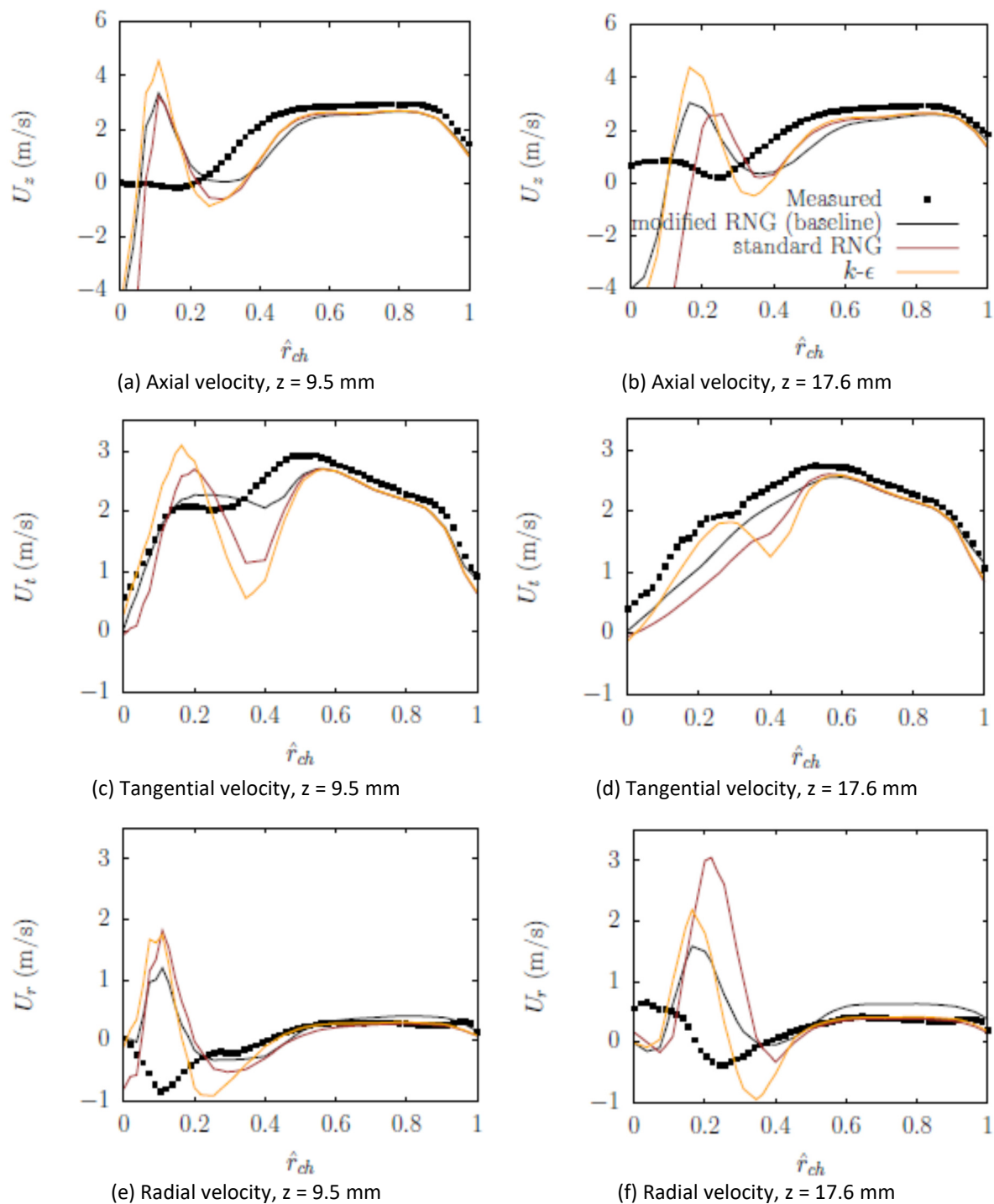


Fig. 2. Validation of reacting gas phase velocity at $z = 9.5$ mm and $z = 17.6$ mm

When the $k - \epsilon$ and standard RNG models are implemented, the far field velocity prediction is similarly accurate to that of the modified RNG model as seen in the coloured curves in Fig. 3(a) to (f). The most apparent effect can be seen in the near field tangential velocity predictions in Fig. 3(c) and (d) where the modified RNG model produces the tangential velocity trend as seen in the experiment whereas the other two models over predict the spray momentum effects even though the droplets do not carry tangential momentum at the time of injection. The variable effects of the spray dynamics on the gas phase flow field using different turbulence models may not be taken as a direct effect of

the spray on turbulence since k and ε transport equations in the present OpenFOAM version do not include the spray source term. However, the increase in the C_2 constant that leads to the increase in the rate of destruction of ε in the modified RNG model may reduce the spray momentum effect on the gas velocity.

The measured volume flux V and the droplet density D which are based on the droplet size and velocity measurement are compared with the predictions of the normalised volume flux \hat{V} and the normalised droplet density \hat{D} respectively. The number of parcels in the reacting case simulation is allowed to converge before the Lagrangian sampling is started to ensure the consistency of a steady spray characteristics prediction. In order to collect enough samples at each radial location, the sampling is done at a rate of 10 kHz for 0.03 s real time. The duration of sampling is considered long enough as the average injection velocity is 20 m/s which allow enough parcels to pass through the probe volume during the sampling duration.

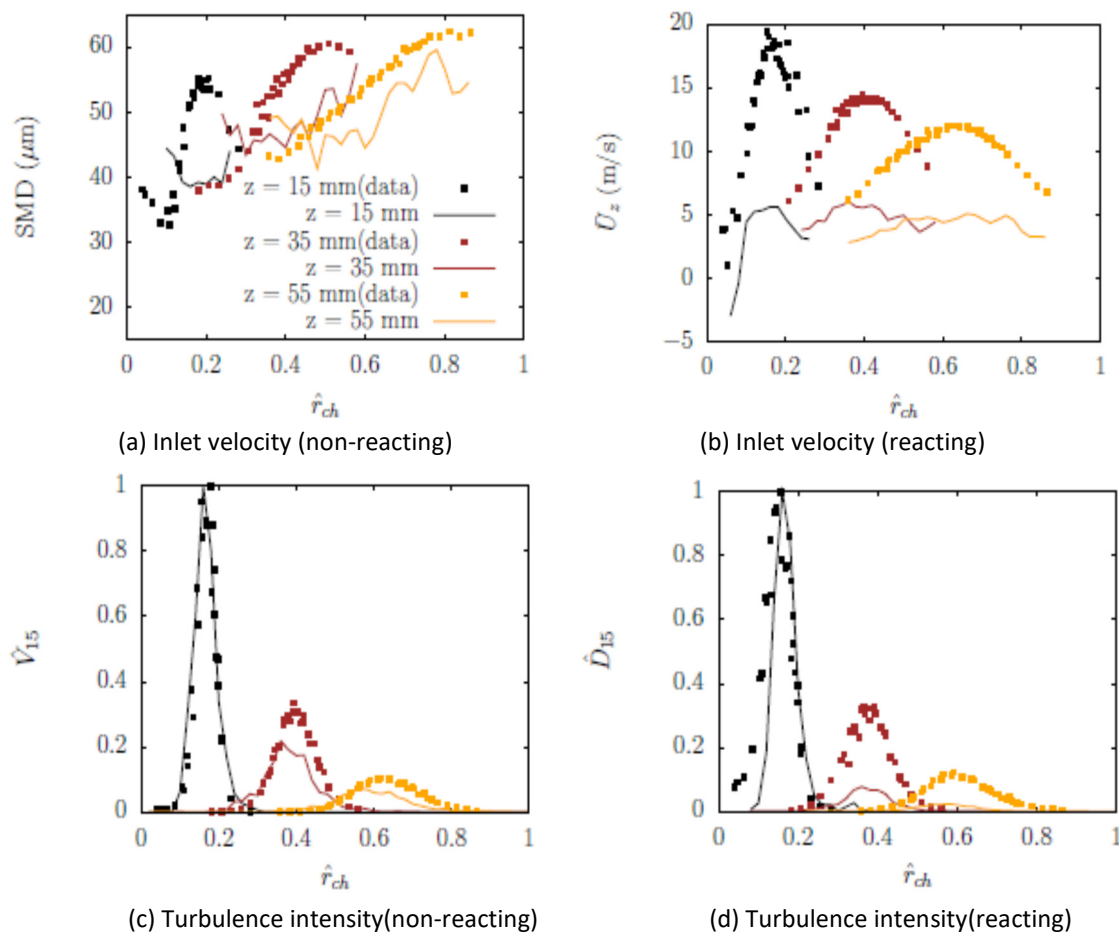


Fig. 3. Spray characteristics validation of the reacting methanol spray.

Figure 4(a) shows the validation of the Sauter mean diameter (SMD) prediction at various axial locations of the baseline case. The prediction reproduces the expansion of the hollow cone spray as seen in the experiment with an increasing SMD in the radial direction. In general, the agreement with the data is satisfactory at $z = 55$ mm where a maximum of 12% error is seen between the measurement and the simulation. A higher degree of under prediction is seen in the near-nozzle region ($z = 15$ mm) which could be due to the over predicted droplet evaporation rate.

Figure 4(b) shows the validation of the mean axial velocity of droplets where a significant under prediction is seen though the parabolic trend of the measured axial velocity is reproduced in the

simulation. The mean injection velocity based on empirical input is implemented at the spray boundary condition, which has been proven to predict the mean axial velocity of a Jet-A1 non-evaporating spray successfully [16]. The drag model of a rigid sphere [12] might over predict the drag in the present simulation which has three times larger droplet size at the spray boundary condition compared to that of the previous non-evaporating spray simulation [16]. The drag model remains in its standard form [10] in the present simulation.

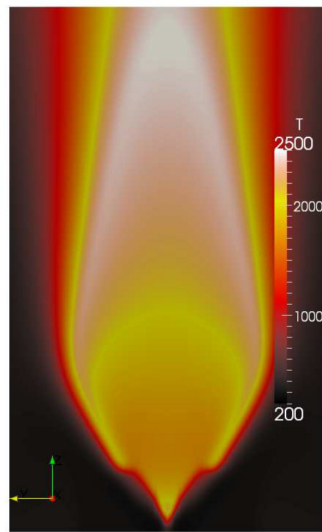
Referring to Fig. 4(c), the prediction of \hat{V}_{15} is compared with that of the measurement. The normalised volume flux $\hat{V}_{15} = V/V_{max,15}$ where V and $V_{max,15}$ are the local volume flux and the maximum volume flux at $z = 15$ mm respectively. The value of $V_{max,15}$ is different in the experiment and the simulation. The prediction of \hat{V}_{15} agrees quite well with the data where the \hat{V}_{15} profile with a maximum value is observed. The maximum \hat{V}_{15} magnitude reduces due to the evaporation downstream. Given that the normalisations of the radial position \hat{r}_{ch} are identical in the simulation and the experiment, the volume flux prediction shows that the cone angle based on the maximum volume flux location is reproduced quite well. Based on the 30% under prediction of the maximum \hat{V} at $z = 35$ mm, it can be inferred that the rate of evaporation is overpredicted which supports the same argument that explains the underprediction of the SMD.

Figure 4(d) shows that the simulation reproduces the droplet density \hat{D}_{15} profile that follows a similar trend to the \hat{V}_{15} profile as seen in the experiment. The normalised droplet density $\hat{D}_{15} = D/D_{max,15}$ where D and $D_{max,15}$ are the local droplet density and the maximum droplet density at $z = 15$ mm respectively. The value of $D_{max,15}$ is different in the experiment and the simulation. However, the \hat{D} reduction rate is over predicted by more than 50% which supports the same argument about the over predicted evaporation rate. The large discrepancy with the experimental data in the peak \hat{D} prediction at $z = 35$ mm signifies the large influence of the small droplets that evaporate at a much higher rate compared to the large ones.

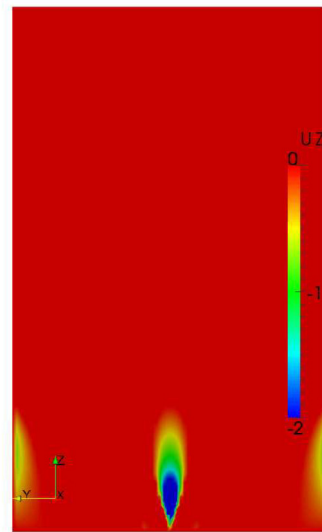
On comparing the profiles of the measured spray characteristics in Fig. 4(a) and (c), the locations of maximum and minimum SMD correspond to the spray region which has low local volume flux. The high and low local volume regions correspond to the linear and non-linear SMD regions respectively. As the spray travels further into the hot region of the flame front, the droplets within the region with low volume flux evaporates rapidly and the SMD profile becomes more linear as seen in Fig. 4(a).

Figures 4 (a) and (c) show the resulting temperature field of the baseline and that of the high reaction rate cases respectively. The general shape of the temperature field remains the same at high reaction rate but the high temperature region is shifted further downstream which can be seen at the top flame brush. A more significant effect of increasing the reaction rate can be seen at the bottom of the flame where the flame lift is shifted downstream, which is quite counter intuitive. The reason for the observed change can be seen in Figs. 4 (b) and (d) where the reverse velocity region produced behind the bluff body at the swirler outlet is weakened and shifted further downstream as the reaction rate is increased. The minor change in the reverse velocity region is enough to cause a change in the spatial temperature distribution near the bottom of the flame. The increase in reaction rate produces an increase in the axial velocity magnitude due to the thermal expansion which weakens the swirl and the reverse velocities. The presence of swirl is seen to produce a more complex response of the combustion solution towards the change in reaction rate.

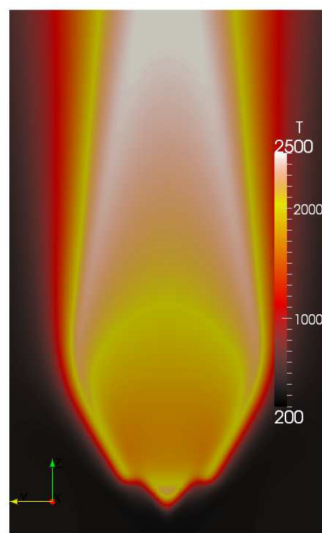
Another computational study [8] found the same effect on the temperature field by reducing A from the baseline case which is the opposite modification to the present study. The study uses the CFD-ACE code with one-step chemistry [8] which could be the cause of discrepancy. Another cause of discrepancy could be due to the use of a different turbulence model (standard RNG model) which might induce a different response of the flow field towards the change in the local heat release rate.



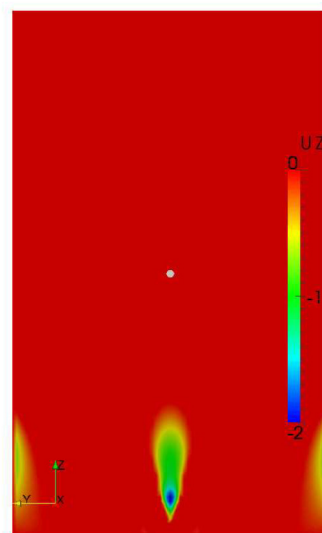
(a) Temperature field of the baseline case



(b) Axial velocity of the baseline case*



(c) Temperature field of the high reaction rate case



(d) Axial velocity of the high reaction rate case*

Fig. 4. Effect of reaction rate on the predicted temperature and the flow field. *The axial velocity scale is modified to highlight the reverse velocity region

4. Conclusions

A validation case of a benchmark methanol spray flame has been done to evaluate the accuracy of the OpenFOAM spray combustion solver. Overall, good agreement between the predictions and the measurements in terms of the global flame shape, global spray structure, gas phase velocity, and spray characteristics is achieved by implementing the empirical spray and gas phase boundary conditions. By increasing C_2 constant in the destruction rate term of ϵ transport equation in the RNG turbulence model, a better prediction of the tangential gas velocity in the near field region is

achieved. Due to the over predicted momentum transfer between the dispersed phase and the gas phase, a large discrepancy is found between the measurement and the prediction of the near field velocity. The variable SMD radial profile is reproduced in the simulation with a maximum error of 12% at $z = 55$ mm. The cone angle based on the location of maximum volume flux is predicted well in the simulation though the rate of droplet reduction is over predicted.

References

- [1] Ramlan, N.U.R.A., Adamabdullah, A., Herzwan, M. "Evaluation of Diesel Engine Performance and Exhaust Emission Characteristics using Waste Cooking Oil." *Journal of Advanced Research in Fluid Mechanics and Thermal Sciences* 12, no. 1 (2015): 11–20.
- [2] James, S., Zhu, J., Anand, M.S. "Large-eddy simulations as a design tool for gas turbine combustion systems." *AIAA journal* 44, no. 4 (2006): 674-686.
- [3] Iaccarino, G., Ooi, A., Durbin, P.A., Behnia, M. "Reynolds averaged simulation of unsteady separated flow." *International Journal of Heat and Fluid Flow* 24, no. 2 (2003): 147-156.
- [4] Sadiki, A., Janicka, J. "Unsteady methods (URANS and LES) for simulation of combustion systems." In *ICHMT DIGITAL LIBRARY ONLINE*. Begel House Inc., 2004.
- [5] Yuan, W., Hansen, A.C. "Computational investigation of the effect of biodiesel fuel properties on diesel engine NO_x emissions." *International Journal of Agricultural and Biological Engineering* 2, no. 2 (2009): 41-48.
- [6] Choi, C.Y., Reitz, R.D. "Modeling the effects of oxygenated fuels and split injections on DI diesel engine performance and emissions." *Combustion science and technology* 159, no. 1 (2000): 169-198.
- [7] Widmann, J.F., Presser, C. "A benchmark experimental database for multiphase combustion model input and validation." *Combustion and Flame* 129, no. 1 (2002): 47-86.
- [8] Crocker, D.S., Giridharan, M.G., Widmann, J.F., Presser, C. "Simulation of Methanol Combustion in the NIST Reference Spray Combustor." *ASME-PUBLICATIONS-HTD* 367 (2000): 95-102.
- [9] Collazo, J., Porteiro, J., Patiño, D., Miguez, J.L., Granada, E., Moran, J. "Simulation and experimental validation of a methanol burner." *Fuel* 88, no. 2 (2009): 326-334.
- [10] Weller, H.G., Tabor, G., Jasak, H., Fureby, C. "A tensorial approach to computational continuum mechanics using object-oriented techniques." *Computers in physics* 12, no. 6 (1998): 620-631.
- [11] Westbrook, Ch.K., Dryer, F.L. "Simplified reaction mechanisms for the oxidation of hydrocarbon fuels in flames." *Combustion science and technology* 27, no. 1-2 (1981): 31-43.
- [12] Kärrholm, F.P. *Numerical modelling of diesel spray injection, turbulence interaction and combustion*. Chalmers University of Technology, 2008.
- [13] Liu, A.B., Mather, D., Reitz, R.D. *Modeling the effects of drop drag and breakup on fuel sprays*. No. TP-930072. Wisconsin Univ-Madison Engine Research Center, 1993.
- [14] Launder, B.E., Spalding, D.B. "The numerical computation of turbulent flows." *Computer methods in applied mechanics and engineering* 3, no. 2 (1974): 269-289.
- [15] Yakhot, V., Orszag, S.A. "Renormalization group analysis of turbulence. I. Basic theory." *Journal of scientific computing* 1, no. 1 (1986): 3-51.
- [16] Widmann, J., Presser, C., Giridharan, M., Crocker, D. "Issues related to spray combustion modelling validation." *AIAA* 363 (2001): 2001.
- [17] Mohd Yasin, M.F. *Modelling of Biodiesel Spray Combustion*. Engineering Department, University of Cambridge, Cambridge, 2014.